# RESEARCH ACTIVITIES

## Theoretical and Computational Molecular Science

It is our goal to develop new theoretical and computational methods based on quantum mechanics, statistical mechanics, and molecular simulation in order to predict and understand the structures, reactions, and functions of molecules in gas, solution, and condensed phases as well as in nano- and bio-systems prior to or in cooperation with experiment.

# Theoretical Study and Design of Functional Molecules: New Bonding, Structures, and Reactions

**Department of Theoretical and Computational Molecular Science**
**Division of Theoretical Molecular Science I**

| | |
|---|---|
| NAGASE, Shigeru | Professor |
| GADRE, Shridhar R. | Visiting Professor |
| JANG, Joonkyung | Visiting Associate Professor* |
| OHTSUKA, Yuki | Assistant Professor |
| TANAKA, Masato | IMS Fellow |
| KATOUDA, Michio | Post-Doctoral Fellow |
| GAO, Xingfa | Post-Doctoral Fellow |
| GUO, Jing-Doing | Post-Doctoral Fellow |
| WANG, Lu | Post-Doctoral Fellow |
| MIYAKE, Toshiko | Post-Doctoral Fellow |
| WON, Jongok | Visiting Scientist† |
| RAHALKAR, Anuja P. | Graduate Student‡ |
| YAMADA, Mariko | Secretary |
| KONDO, Naoko | Secretary |


In theoretical and computational chemistry, it is an important goal to develop functional molecules prior to or in cooperation with experiment. Thus, new bonds and structures provided by heavier atoms are investigated together with the reactivities. In addition, chemical modification and properties of large molecules are investigated to develop functional nanomolecular systems. Efficient computational methods are also developed to perform reliable quantum chemistry calculations for small and large molecular systems.

## 1. Efficient Parallel Algorithm of Second-Order Møller-Plesset Perturbation Theory with Resolution-of-Identity Approximation (RI-MP2)[1)]

Density functional theory (DFT) is widely used to calculate large molecules as well as small molecules because of its accuracy and low computational cost. However, the generally used DFT methods fail to describe noncovalent interactions that play an essential role in host-guest molecules, self-assembly, molecular recognition, and three-dimensional structures of proteins, and usually underestimate reaction barriers. Therefore, many attempts have been made to develop new functionals. However, no widely applicable method has emerged yet.

Second-order Møller-Plesset perturbation theory (MP2) is the simplest and effective method that accounts for electron correlation effects important for noncovalent interactions and reaction barriers. MP2 is also helpful for checking DFT results. Despite these advantages, the formal scaling of MP2 calculations is $O(n^5)$ (n is the number of basis functions), much higher than that of DFT calculations. We have recently developed a new parallel algorithm of MP2 calculations. Despite this new algorithm, MP2 calculations of huge molecules are considerably time-consuming and require very large sizes of fast memory and hard disk. Therefore, we have developed an efficient parallel algorithm of RI-MP2 calculations to reduce highly the computational cost as well as the sizes of memory and disk by employing the resolution-of the identity (RI) approximation for two-electron repulsion integrals. The parallel algorithm aims at reducing I/O overheads and achieving good load balancing.

Test parallel calculations were carried out using 6-31G* and 6-311G basis sets for taxol ($C_{47}H_{51}NO_{14}$), valinomycin ($C_{54}H_{90}N_6O_{18}$), two-layer nanographene sheets ($C_{192}H_{28}$), and the noncovalent complex of $C_{60}$ and $C_{60}H_{28}$. All the RI-MP2 calculations were performed on a Linux cluster of 3.2 GHz EM64T Pentium 4 processors connected by a Gigabit Ethernet network. These calculations confirm the high parallel efficiency of the developed algorithm. For taxol, the speedup, defined as the ratio of elapsed time, was almost linear, 27.0 (6-31G*) and 29.6 (6-311G*) for 32 processors. For valinomycin with the larger number of basis functions, super-linear scaling was achieved, the speedup being 36.6 (6-31G*) and 34.8 (6-311G*) for 32 processors. As the calculations of the noncovalent complex of $C_{60}$ and $C_{60}H_{28}$ show (Figure 1), the high parallel efficiency is kept up to 64 CPU cores. The parallel efficiency depends on the speed of network communication because the amount of network communication increases linearly as the number of processors. It is expected that the high parallel efficiency is kept up to much more processors when more efficient network communication is employed. As shown by the RI-MP2 calculation of two-layer nanographene sheets with the 6-311 G* basis set (3,932 basis functions), only 2.3 GB memory per processor and a total of 228 GB disk are required, unlike the MP2 calculation that requires 14.6 GB memory and a total of 7.9 TB disk. In addition, RI-MP2 energies deviate from MP2 energies only by 1-3 mHartree.

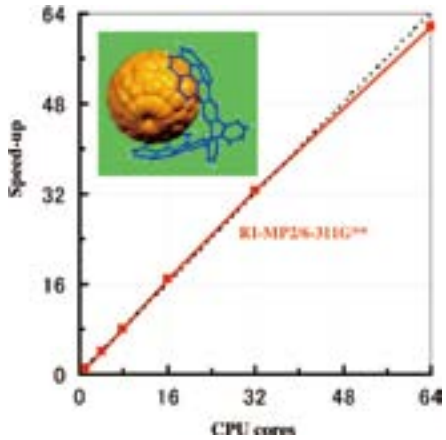


**Figure 1.** The RI-MP2 parallel calculations of the complex of $C_{60}$ and $C_{60}H_{20}$.

## 2. Computational Approach to the Structures, Reactions, and Functionalization of Large Molecules

There has been much interest in silicon-silicon triply bonded compounds. Therefore, the structure and properties of 1,2-diaryldisilyne (ArSi≡SiAr), isolated by introducing bulky aryl groups (Ar = $C_6H_2$-2,6{$CH(SiMe_3)_2$}$_2$-4-$C(SiMe_3)_3$), were investigated by theoretical calculations.[2,3] The mechanisms of unique reactions of $R^{Si}Si{\equiv}SiR^{Si}$ protected by bulky silyl groups ($R^{Si}$ = $Si^iPr${$CH(SiMe_3)_2$}$_2$) were theoretically disclosed.[4] In addition, neutral organogallium aryl dimeres and monomers were investigated to characterize the gallium-gallium bonds in digallenes and digallynes.[5]

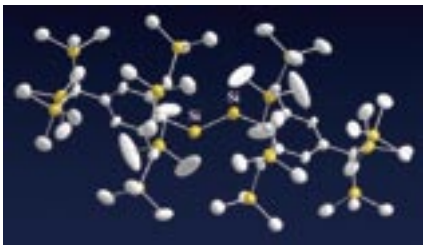

Endohedral metallofullerenes are of great interest in developing functional nanomolecules. It is an important task to observe the $^{13}C$ NMR chemical shifts of metal carbides in $Sc_2C_2@C_{82}$, $Sc_2C_2@C_{84}$, and $Sc_3C_2@C_{80}$ in an attempt to provide insight into its electronic and magnetic properties. The $^{13}C$ NMR chemical shifts were theoretically predicted and experimentally confirmed using $^{13}C$-enriched samples.[6] In addition, calculations were performed for the radical coupling reactions of paramagnetic endohedral metallofullerenes,[7] anisotropic behavior of anionic carbene derivatives,[8] and missing metallofullerenes.[9]

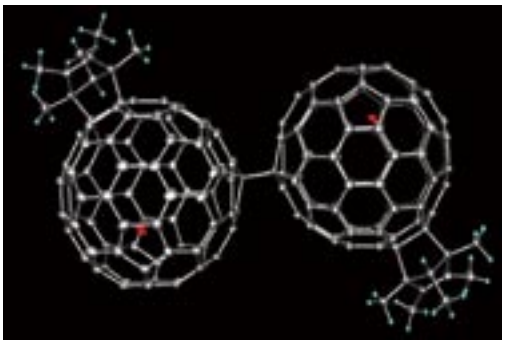

Nanographene (NG) has attracted great interest as the new generation of carbon electronics. We predicted how the oxidation unzipping of stable NG leads to spin-rich fragments in an attempt to realize NG-based molecular magnets.[10]

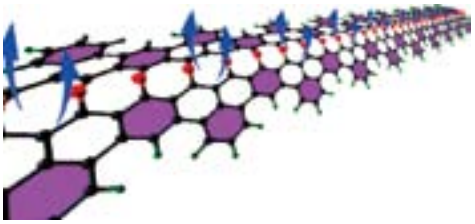

### References


1) M. Katouda and S. Nagase, *Int. J. Quant. Chem.* **109**, 2121–2130 (2009).
2) T. Sasamori, K. Hironaka, Y. Sugiyama, N. Takagi, S. Nagase, Y. Hosoi, Y. Furukawa and N. Tokitoh, *J. Am. Chem. Soc.* **130**, 13856–13857 (2008).
3) T. Sasamori, J. S. Han, K. Hironaka, N. Takagi, S. Nagase and N. Tokitoh, *Pure Appl. Chem.* in press.
4) K. Takeuchi, M. Ichinohe, A. Sekiguchi, J. -D. Guo and S. Nagase, *Organometallics* **28**, 2658–2660 (2009).
5) Z. Zhu, R. C. Fischer, B. D. Ellis, E. Rivard, W. A. Merrill, M. M. Olmstead, P. P. Power, J. -D. Guo, S. Nagase and L. Pu, *Chem. Eur. J.* **15**, 5263–5272 (2009).
6) Y. Yamada, K. Nakajima, T. Wakahara, T. Tsuchiya, M. O. Ishitsuka, Y. Maeda, T. Akasaka, M. Waelchli, N. Mizorogi and S. Nagase, *Angew. Chem., Int. Ed.* **47**, 7905–7908 (2008).
7) Y. Takano, A. Yomogida, H. Nikawa, M. Yamada, T. Wakahara, T. Tsuchiya, Y. Maeda, T. Akasaka, T. Kato, Z. Slanina, N. Mizorogi and S. Nagase, *J. Am. Chem. Soc.* **130**, 16224–16230 (2009).
8) Y. Takano, M. Aoyagi, M. Yamada, H. Nikawa, Z. Slanina, N. Mizorogi, M. O. Ishitsuka, T. Tsuchiya, Y. Maeda, T. Akasaka, T. Kato and S. Nagase, *J. Am. Chem. Soc.* **131**, 9340–9346 (2009).
9) H. Nikawa, Y. Yamada, B. Gao, N. Mizorogi, Z. Slanina, T. Tsuchiya, T. Akasaka, K. Yoza and S. Nagase. *J. Am. Chem. Soc.* **131**, 10950–10954 (2009).
10) X. Gao, L. Wang, Y. Ohtsuka, D. -E. Jiang, Y. Xhao, S. Nagase and Z. Chen, *J. Am. Chem. Soc.* **131**, 9663–9669 (2009).



* Present Address; Present Address; Department of Nanomaterials Engineering, Pusan National University, Miryang 627-706, Korea
† Present Address; Department of Applied Chemistry, Sejong University, Seoul 143-747, Korea
‡ Present Address; Department of Chemistry, University of Pune, Pune 411007, India

# Electronic Structure and Electron-Nuclear Dynamics of Molecules in Contact with an Electron Reservoir

**Department of Theoretical and Computational Molecular Science**
**Division of Theoretical Molecular Science I**

| | |
|---|---|
| NOBUSADA, Katsuyuki | Associate Professor |
| YASUIKE, Tomokazu | Assistant Professor |
| IWASA, Takeshi | JSPS Post-Doctral Fellow |
| KUBOTA, Yoji | Post-Doctoral Fellow |
| NODA, Masashi | Post-Doctoral Fellow |
| YAMADA, Mariko | Secretary |


Electronic structures and electron dynamics of molecules or nanostructured materials in contact with an electron reservoir play important roles in heterogeneous catalysis, surface photochemistry, and also electrochemistry. We have developed theoretical methods to calculate electronic structures of adsorbate-surface systems and electron-nuclear dynamics on their electronic potential-energy-surfaces. We have also investigated exciton transfer dynamics in an array of quantum dot. Furthermore, a generalized theoretical description of a light-matter interaction beyond a dipole approximation is developed on the basis of the multipolar Hamiltonian with the aim of understanding the near-field excitation of molecules at the 1 nm scale.

## 1. Photoinduced Coherent Adsorbate Dynamics on a Metal Surface: Nuclear Wave-Packet Simulation with Quasi-Diabatic Potential Energy Curves Using an Open-Boundary Cluster Model Approach[1)]

We present a nuclear wave-packet simulation of photo-induced coherent adsorbate dynamics on a metal surface with quasi-diabatic potential energy curves obtained from our recently developed open-boundary cluster model approach. Photoexcitation to the resonant adsorbate state and the subsequent ultrafast decay to the electronically excited substrate states were found to cause a coherent vibration of the adsorbate on the metal surface. This process competes with a Raman scattering process, which is generally believed to explain the coherent adsorbate vibration. These two mechanisms induce vibrations with a common frequency, and therefore cannot be distinguished from each other in a frequency-domain experiment. However, they can be distinguished by determining the initial vibrational phase through a time domain experiment such as ultrafast pump-probe spectroscopy. We further demonstrate that for near-resonant excitation the oscillation amplitude induced by our proposed mechanism largely exceeds the amplitude due to the Raman mechanism.

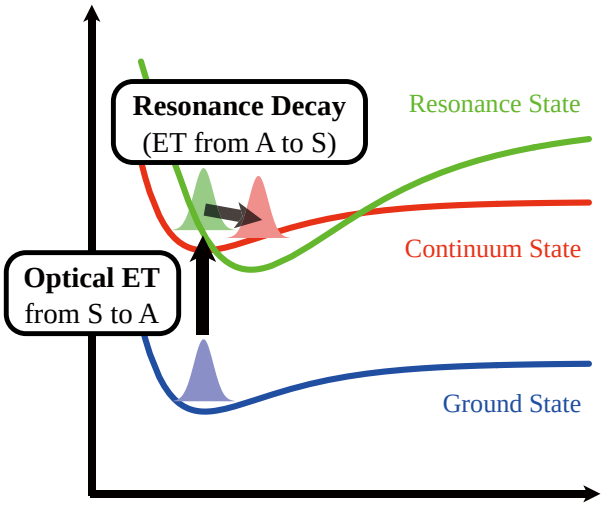


**Figure 1.** Schematic diagram of the TAM mechanism of causing coherent vibrational motion of the adsorbate on the continuum state.

## 2. Nonuniform Light-Matter Interaction Theory for Near-Field-Induced Electron Dynamics

A generalized theoretical description of a light-matter interaction beyond a dipole approximation is developed on the basis of the multipolar Hamiltonian with the aim of understanding the near-field excitation of molecules at the 1 nm scale. The theory is formulated for a system consisting of a molecule and a near-field, where a nonuniform electric field plays a crucial role. The nonuniform light-matter interaction is expressed in terms of a spatial integral of the inner product of

the total polarization of a molecule and an electric field so that the polarization is treated rigorously without invoking the conventional dipole approximation. A nonuniform electronic excitation of a molecule is demonstrated by solving a time-dependent Kohn-Sham equation in real-space and real-time with an implementation of the nonuniform light-matter interaction. The computations are performed to a linear chain molecule of dicyanodiacetylene ($NC_6N$). The nonuniform electronic excitation clearly shows inhomogeneous electron dynamics in sharp contrast to the dynamics induced by a uniform electronic excitation under the dipole approximation. Despite the inversion symmetry of $NC_6N$, the nonuniform excitation generates even harmonics in addition to the odd ones. Higher-order nonlinear optical response and quadrupole excitation are also observed.

## 3. Applicability of Site-Basis Time-Evolution Equation for Thermalization of Exciton States in a Quantum Dot Array[2)]

We verify the practical applicability of the conventional site-basis time-evolution equation to exciton transfer processes in a quantum-dot array model. The time-evolution equation has proved to work under the rather limited conditions of the zero temperature limit and/or a minimal two-dot system. The computed results dramatically change with the temperature, the number of quantum dots, and the intensity of transition rates between adjacent sites. This is due to the fact that the higher-order perturbation terms, which are neglected in deriving the site-basis equation, have a great influence on the exciton dynamics. We found that the thermal relaxation can be suppressed by controlling the dot size and interdot distance.

## 4. Oscillator Strength Distribution of $C_{60}$ in the Time-Dependent Density Functional Theory[3)]

An oscillator strength distribution of the fullerene $C_{60}$ molecule is calculated in the time-dependent density functional theory. A real-time method is employed to obtain the spectrum of a wide energy region extending up to 120 eV. The orbitals are expressed on the uniform grid points in the three-dimensional Cartesian coordinates inside a large cubic box area. The calculated distribution shows an intense peak centered at around 20 eV, accompanying a number of sharp structures on it up to 35 eV. Absolute values and gross features of the oscillator strength distribution are in reasonable agreement with measurements.

## 5. Thiolated Gold Nanowires: Metallic *versus* Semiconducting[4)]

Tremendous research efforts have been spent on thiolated gold nanoparticles and self-assembled monolayers of thiolates on gold, but thiolated gold nanowires have received almost no attention. Here we computationally design two such one-dimensional nanosystems by creating a linear chain of Au icosahedra, fused together by either vertex sharing or face sharing. Then neighboring Au icosahedra are bridged by five thiolate groups for the vertex-sharing model and three RS Au SR motifs for the face-sharing model. We show that the vertex-sharing thiolated gold nanowire can be made either semiconducting or metallic by tuning the charge, while the face-sharing one is always metallic. We explain this difference between the two nanowires by examining their band structures and invoking a previously proposed electron-count rule. Implications of our findings for previous experimentation of gold nanowires are discussed, and a potential way to make thiolated gold nanowires is proposed.

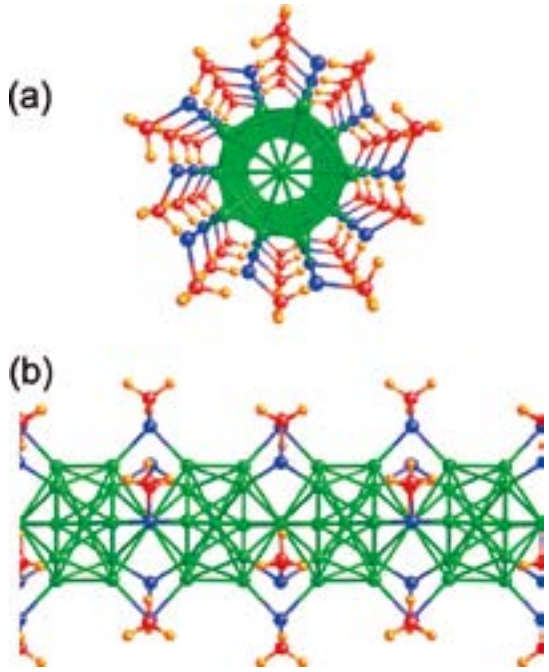


**Figure 2.** Vertex-sharing icosahedral thiolated gold nanowire: (a) viewed along the wire; (b) side view. Au, green; S, blue; C, red; H, orange.

### References

1) T. Yasuike and K. Nobusada, *Phys. Rev. B* **80**, 035430 (8 pages) (2009).
2) Y. Kubota and K. Nobusada, *J. Phys. Soc. Jpn.* **78**, 114603 (7 pages) (2009).
3) Y. Kawashita, K. Yabana, M. Noda, K. Nobusada and T. Nakatsukasa, *THEOCHEM* **914**, 130–135 (2009).
4) D. -E. Jiang, K. Nobusada, W. Luo and R. L. Whetten, *ACS NANO* **3**, 2351–2357 (2009).

# Advanced Electronic Structure Theory in Quantum Chemistry

**Department of Theoretical and Computational Molecular Science**
**Division of Theoretical Molecular Science I**

| | |
|---|---|
| YANAI, Takeshi | Associate Professor |
| KURASHIGE, Yuki | Assistant Professor |
| MIZUKAMI, Wataru | Graduate Student |
| YAMADA, Mariko | Secretary |


Aiming at predictive computational modelings of molecular electronic structures with *ab initio* quantum chemistry calculations, our scientific exploration is to establish a cutting-edge theoretical methodology that allows one to compute accurately and efficiently the complex electronic structures, in which strongly-interacting electrons play a crucial role to characterize the nature of molecules. The complicated electronic structures can be handled accurately with the multi-reference theory, which deals with multiple important electronic configurations on equal footing. However, with the standard multireference methods such as the complete active space self-consistent field (CASSCF), the tractable size of the reference space is limited to small active space because the complexity of the calculations grows exponentially with the reference size. The existing multireference methods are nevertheless usefully applied to chemical theory problems such as exploring chemical reactions of bonding, dissociation and isomerization along the reaction coordinates, electronically excited states, unstable electronic structures of radical systems, and multiple covalent bindings in molecular metal complexes, *etc*. Our resultant works to be reported here are (1) to develop a type of the multireference correlation model named Canonical Transformation (CT) theory, which can efficiently describe short-range dynamic correlation on top of the multi-configurational staring wave function, and (2) to construct the extensive complete active space self-consistent field (CASSCF) method combined with *ab initio* density matrix renormalization group (DMRG) method for making unprecedentedly larger active spaces available for the CASSCF calculations.

## 1. High-Performance *ab initio* Density Matrix Renormalization Group Method Multireference Application for Metal Compounds[1)]

The density matrix renormalization group (DMRG) algorithm has recently attracted significant attention as a robust quantum chemical approach to multireference electronic structure problems in which a large number of electrons have to be highly correlated in a large-size orbital space. It can be seen as a substitute for the exact diagonalization method that is able to diagonalize large-size Hamiltonian matrices. It comprises only a polynomial number of parameters and computational operations, but is able to involve a full set of the Slater determinants or electronic configurations in the Hilbert space, of which the size nominally scales exponentially with the number of active electrons and orbitals. In this work, we have presented a new efficient and parallelized implementation of the DMRG algorithm that is oriented towards applications for poly-nuclear transition metal compounds. The difficulty in DMRG calculations for these systems lies in the large active space and the non-1D nature of the electron correlation. A straightforward extension of the DMRG algorithm has been proposed with further improvements and aggressive optimizations to allow its application with large multireference active space, which is often demanded for metal compound calculations. Special efficiency is achieved by making better use of sparsity and symmetry in the operator and wavefunction representations. By accomplishing computationally intensive DMRG calculations, the authors have found that a large number of renormalized basis states are required to represent high entanglement of the electron correlation for metal compound applications, and it is crucial to adopt auxiliary perturbative correction to the projected density

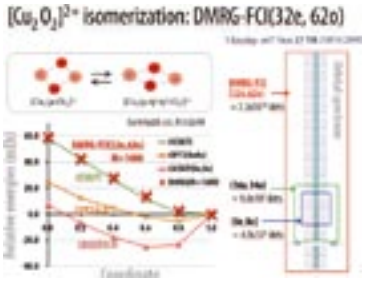


**Figure 1.** DMRG-FCI application to the potential curve of $Cu_2O_2$ isomerization, which is recently under hot debate. The behaviors of the single reference calculations and those of the multireference calculations exhibit clear differences. For this problem, we modeled a fairly large orbital space (32e,62o) to execute the DMRG diagonalization with.It has been shown thatDMRG energies nearly overlap with CCSD(T) results..

matrix during the DMRG sweep optimization in order to attain proper convergence to the solution. Potential energy curve calculations for the $Cr_2$ molecule near the known equilibrium precisely predicted the full configuration interaction (FCI) energies with a correlation space of 24 electrons in 30 orbitals (denoted by (24e,30o)). The energies are demonstrated to be accurate to 0.6 $mE_h$ (the error from the extrapolated best value) when as many as ten thousand renormalized basis states are employed for the left and right DMRG block representations. The relative energy curves for $[Cu_2O_2]^{2+}$ along the isomerization coordinate were obtained from DMRG and other correlated calculations, for which a fairly large orbital space (32e,62o) is modeled as a full correlation space (Figure 1). The DMRG prediction nearly overlaps with the energy curve from the coupled-cluster with singles, doubles and perturbative triples (CCSD(T)) calculations, while the multireference complete active space self-consistent field (CASSCF) calculations with the small reference configuration (8e,8o) are found to overestimate the biradical character of the electronic state of $[Cu_2O_2]^{2+}$, according to the one-electron density matrix analysis.

## 2. DMRG-CASSCF: Spin States of Poly-Carbene[2)]

Posing the multireference problems in quantum chemistry, the complex electronic structures troubling the problems ought to be described by handling multiple electronic configurations, several of which should be equally important in the description. We have recently presented an extensively large-scale CASSCF approach, which is realized by implementing the orbital optimization with the density matrix renormalization group (DMRG) wavefunction (DMRG-CASSCF). By virtue of the compact nature of the DMRG wavefunction, which provides an efficient description of the strongly correlated electronic structures, the DMRG-CASSCF approach enables us to handle much larger active spaces than are possible with the traditional CASSCF algorithm. Using the DMRG-CASSCF method, we investigated the spin states of poly(phenyl)carbenes (Figure 2). These molecules involve a characteristic electronic structure, and the higher-spin states are known to be more stable than the lower-spin states. We examined stability of high-spin state by computing highest and singlet spin states. The table shows energy gaps of 1,2,3-carbene between highest and singlet spin states. For comparison, reference numbers are computed with several single-reference (mean-field + perturbation) methods. In DMRG-CASSCF on 3-carbene, a large CAS(30,30) was used for active space. As expected, all the calculations predicted that high-spin states are more stable than singlet state. However, in terms of the energy gaps, we observed surprisingly large discrepancy between single-reference methods and DMRG-CASSCF. Electronic structure of carbene sites can be represented in sp2 hybridization. Then the high-spin state is described as parallel spins occupying sp2 and $p_z$ orbitals. This description is consistently observed in one-electron density matrix elements of DMRG-CASSCF as well as single determinant wavefunctions. For singlet state, however, as can be seen in the electron density elements, DM RG-CASSCF and single-determinant method chose different configuration. It is found that the single-reference methods describe the lone pair configuration, while DMRG-CASSCF chose this biradical configuration as the stable singlet state. For this reason, DMRG-CASSCF stabilizes the description of the singlet state, and thus the small energy gaps are estimated.

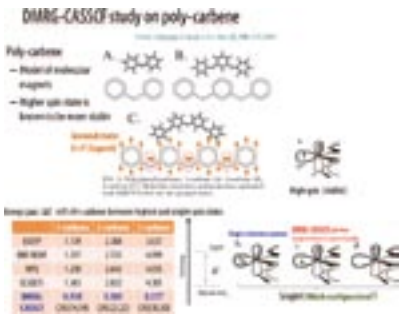


**Figure 2.** DMRG-CASSCF study of poly(phenyl) carbene. This molecule involves a characteristic electronic structure, and the high-spin state is known to be more stable. For 3-carbene, the septet state is thought to be the most stable spin state where you see there are parallel spins on three carbene sites. The table shows energy gaps of 1,2,3-carbene between highest and singlet spin states. For comparison, reference numbers are computed with several single-reference methods.

## 3. Canonical Transformation (CT) Theory for Efficient Multireference Method[3–4)]

We have been developing a many-body technique based on canonical transformation (CT) for realizing large-scale multi-reference calculations for the purpose of attaining the chemical accuracy, for which dynamical correlations are described by using cluster expansion on top of muticonfigurational setting (*e.g.* DMRG-CASSCF). We are working on extending the implementation to the wider applications in terms of tractable size of molecules of target. The ongoing reimplementation fixes some of problems in the extant implementation that relies on infinite computer memory. We have demonstrated the recent application of CT to the description of an energy curve along the isomerization coordinate between bis and peroxo cores of $Cu_2O_2^{2+}$.

### References

1) Y. Kurashige and T. Yanai, *J. Chem. Phys.* **130**, 234114 (2009).
2) T. Yanai, Y. Kurashige, D. Ghosh and G. K-L. Chan, *Int. J. Quantum Chem.* **109**, 2178 (2009).
3) E. Neuscamman, T. Yanai and G. K-L. Chan, *J. Chem. Phys.* **130**, 124102 (2009).
4) G. K-L. Chan, J. J. Dorando, D. Ghosh, J. Hachmann, E. Neuscamman, H. Wang and T. Yanai, *Frontiers in Quantum Systems in Chemistry and Physics*, S. Wilson *et al.*, Eds., Springer, **Vol. 18**, pp. 49–64 (2008).

### Award

YANAI, Takeshi; The Wiley-International Journal of Quantum Chemistry Young Investigator Award (The 49th Sanibel Symposium, 2009).

# Developing the Statistical Mechanics Theory of Liquids in Chemistry and Biophysics

**Department of Theoretical and Computational Molecular Science**
**Division of Theoretical Molecular Science II**

| | |
|---|---|
| HIRATA, Fumio | Professor |
| CHONG, Song-ho | Assistant Professor |
| YOSHIDA, Norio | Assistant Professor |
| MARUYAMA, Yutaka | Post-Doctoral Fellow |
| MIYATA, Tatsuhiko | Post-Doctoral Fellow |
| ISHIZUKA, Ryosuke | Post-Doctoral Fellow |
| PHONGPHANPHANEE, Saree | Post-Doctoral Fellow |
| KIYOTA, Yasuomi | Graduate Student |
| SUETAKE, Yasumi | Secretary |
| KONDO, Naoko | Secretary |
| YAMADA, Mariko | Secretary |


We have been developing a new theory for the molecular recognition by protein based on the statistical mechanics of liquids, or the 3D-RISM/RISM theory. The theory has demonstrated its amazing capability of "predicting" the process from the first principle.[1–3] However, what we have investigated so far is an entirely equilibrium process both in protein conformation and solvation.

Recently, we have started to incorporate the conformational fluctuation of protein into the molecular recognition process in two ways. The first of those is a "static" one in which we just shake the protein conformation to find the local minimum of the free energy surface by the combined 3D-RISM/RISM with conformational sampling algorithms, and to see if one can find the distribution of a guest molecule in the recognition site.[4] The other method is to take the "dynamic" fluctuation of protein conformation into account. The process can be described by hybridized 3D-RISM/RISM with the generalized Langevin theories.[5] The methodology is currently under construction, and some prospective view of the theory will be presented in the lecture.

## 1. 3D-RISM/RISM Studies on the Dissociation Pathway of CO in Myoglobin[6]

Myoglobin (Mb) is a globular protein which has important biological functions, or oxygen storage. Due to its biochemical function, many researchers have made intensive efforts to identify the escaping pathway of the ligand, experimentally and theoretically.[7]

Among many unresolved questions with respect to the CO escaping pathway, the dependence of the pathway on Xe concentration has recently been highlighted by Terazima based on the time-resolved partial molar volume (PMV) measured with the transient grating spectroscopy. The experimental results indicate that CO is trapped at the Xe site before escaping to solvent at room temperature. The difference of Xe and CO affinity of each Xe trapping site makes the CO escaping pathway different depending on Xe concentration. It is believed that the dissociated CO escapes to the solvent through the Xe1 trapping site under the Xe-free condition, dominantly, while CO escapes through the Xe4 site in a Xe-rich solution.

Shown in Figure 1 is the 3D-distribution of CO in the four Xe-sites calculated from 3D-RISM in the ternary mixture composed of water, Xe, and CO. It is apparent that each Xe-site has some affinity to a CO molecule. The comaprison of the population of CO and Xe in each Xe-site at high concentration revealed that Xe has greater affinity to the Xe1 site than CO, while CO is dominant in the Xe4-site.

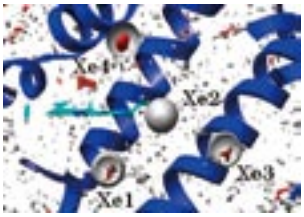


**Figure 1.** CO distribution in the Xe-sites: red, O; gray, C.

**Table 1.** The partial molar volume of the different association state of the CO-Mb complex. ($\Delta V_1$ = (Mb:CO) – (MbCO), $\Delta V_2$ = (Mb+CO) – (Mb:CO), and $\Delta V_{total}$ = (Mb+CO) – (MbCO)).

| models | PMV[cm$^3$/mol] |
|---|---|
| MbCO | 9029.0 |
| Mb:CO(Xe1) | 9030.4 |
| Mb:CO(Xe4) | 9032.8 |
| MB+CO | 9019.6 |

| | Xe1 | Xe4 | (exptl.[7]) |
|---|---|---|---|
| $\Delta V_1$ = | 1.4 | 3.8 | (3±1) |
| $\Delta V_2$ = | –10.8 | –13.2 | (–12.6±1.0) |
| $\Delta V_{total}$ = | –9.4 | –9.4 | (–10.7±0.5) |

(MbCO, CO bound at the Heme; Mb:CO(Xe1), CO is bound at the Xe1 site: Mb:CO(Xe4), CO is bound at the Xe4-site; MB+CO, CO is dissociated from Mb.)

In order to examine the hypothesis made by Terazima with respect to the escaping pathway, we have calculated PMV of the CO-Mb complexes in each of which a CO molecule is explicitly bound in one of the Xe-sites. The results are shown

in Table 1. As is obvious from the table, the theoretical results for Mb:CO(Xe4) show much better agreement with the experiment, indicating that CO escapes from the Xe4-site. The hypothesis made by Terazima is thus verified by the theory.

## 2. An Attempt toward the Generalized Langevin Dynamics Simulation[5)]

It has been five decades since the molecular simulation scored its first step in the study of liquids and solutions. Accelerated by the increasing power of computer, the method has been enjoying the status of a standard tool to explore the molecular aspects of physical, chemical, and biological processes in liquids and solutions. However, the method is facing high barriers which may not be overcome by the improvement of computing power alone. One of those is the large and slow fluctuations taking place in a protein in solutions, which touches the zero wavelength and frequency limits. Straightforward applications of the molecular simulation to the limits are in danger to end up with an "animation" or a "science fiction."

In this report, we have attempted a new step toward the molecular dynamics simulation which is not based on the Newton equation, but on the generalized Langevin theory, in which all the degrees of freedom concerning the solvent molecules are "coarse-grained" or "projected" in term of the pair correlation functions. Choosing the coordinates $\boldsymbol{R}$ of protein atoms and the density field ρ of solvent atoms, as well as their conjugated momentum, as dynamic variables in the phase space, we have derived the generalized Langevin equations for protein dynamics in solutions.

$$\frac{d\mathbf{R}(t)}{dt} = \frac{\mathbf{P}(t)}{M}$$

$$\frac{d\mathbf{P}(t)}{dt} = -k_B T\mathbf{L}^{-1}\cdot\mathbf{R}(t) - \frac{1}{Mk_BT}\int_0^t ds\left\langle \mathbf{W}e^{i(t-s)QL}\right\rangle\cdot\mathbf{P}(s) + e^{itQL}\mathbf{W}$$

$$\frac{d\rho_k(t)}{dt} = ikJ_k^L(t)$$

$$\frac{dJ_k^L(t)}{dt} = \frac{ikk_BT}{mS_k}\delta\rho_k(t) - \frac{m}{Nk_BT}\int_0^t \left\langle R_{-k}e^{i(t-s)QL}R_k\right\rangle J_k^L(s) + e^{itQL}f_k$$

where $\boldsymbol{R}$ and $\boldsymbol{P}$ denote the coordinates and conjugated momenta of protein atoms, ρ and $J$ the density and momentum field of solvent atoms, respectively. The first two equations describe the dynamics of protein, while the last two are concerned with the solvent dynamics. However, they should be solved simultaneously, since the equations are closely coupled each other. It is our plan to solve the equation in the way just as is done in the molecular dynamic simulation, or the numerical integration of the equation.

The equations for protein have a typical expression of the original Langevin equation, but each term in the right hand side has a microscopic description in contrast to the original one. The first term is related to the variance-covariance matrix of mean square displacement of protein, which signifies the conformational fluctuation of the molecule. The factor $k_BT\boldsymbol{L}^{-1}$ is related to a frequency matrix of the fluctuation, or the variance-covariance matrix (<Δ$R$Δ$R$>)), diagonalization of which gives rise to an "effective normal mode" of the fluctuation. The second term is the damping or drag term. In the original Langevin equation, this term is local in time, and is described by the phenomenological expression such as the Oseen tensor which models the hydrodynamic interactions. The third term stands for the "random" force acting on the solute, which of course is orthogonal to the dynamic variables at time zero.

It is a highly nontrivial problem to solve the equation by means of the numerical integration. Our working hypothesis to solve the equations is following.

(1) For each time step Δ$t$, the protein structure is at "local equilibrium," and the fluctuation around the equilibrium follows the "central limiting theorem," or the "Gaussian fluctuation."

(2) By virtue of the Gaussian fluctuation, the variance-covariance matrix (<Δ$R$Δ$R$>) can be the second derivative of the free energy of protein (conformational energy + solvation free energy) with respect to protein atom positions.

(3) The solvation free energy of protein and its derivatives can be evaluated from the 3D-RISM theory. (The variance-covariance matrix (<Δ$R$Δ$R$>) is proportional to the second derivative.

(4) The time step Δ$t$ of integration should be sufficiently large so that the central limiting theorem is valid, while it should be small enough so that the memory term can be approximated with a short time memory.

(5) The perturbation onto solution from protein can be treated by a renormalized potential or the direct correlation functions.

There is another concern in the actual implementation of the theory to the computational science. Each time step of the numerical integration requires the solution of the 3D-RISM equation, which has been notorious with respect to the computational time. For example, when the equation was first solved for protein about five years ago, it took "a month" by ordinary workstations to get the 3D-distribution around "one" conformation of the solute. It was essentially due to the 3D-FFT program which is notorious about the parallelization. If it is the case, the new approach described above is useless, because the simulation requires thousands of steps to explore a meaningful region of the conformational space. However, we could have made a dramatic progress during the year of 2009, thanks to the collaboration with the computer scientists in Tsukuba: The current achievement is "a minute per a conformation" of protein with T2K in Tsukuba.

### References


1) F. Hirata, *Molecular Theory of Solvation*, Kluwer; Dordrecht, Netherlands (2003).

2) A. Kovalenko and F. Hirata, *J. Chem. Phys.* **110**, 10095–10112 (1999).

3) T. Imai, R. Hiraoka, A. Kovalenko and F. Hirata, *J. Am. Chem. Soc. (Communication)* **127**, 15334–15335 (2005).

4) T. Miyata and F. Hirata, *J. Comput. Chem.* **29**, 872 (2007).

5) B. Kim, S-H. Chong, R. Ishizuka and F. Hirata, *Cond. Matt. Phys.* **11**, 179 (2008).

6) Y. Kiyota, R. Hiraoka, N. Yoshida, Y. Maruyama, T. Imai and F. Hirata, *J. Am. Chem. Soc. (Communication)* **131**, 3852 (2009).

7) M. Sakakura, S. Yamaguchi, N. Hirota and M. Terazima, *J. Am. Chem. Soc.* **123**, 4286 (2001).

# Theory of Nonequilibrium Quantum Dynamics and Transport

**Department of Theoretical and Computational Molecular Science**
**Division of Theoretical Molecular Science II**

| | |
|---|---|
| YONEMITSU, Kenji | Associate Professor |
| YAMASHITA, Yasufumi | Assistant Professor* |
| TANAKA, Yasuhiro | IMS Research Assistant Professor |
| MIYASHITA, Satoshi | Post-Doctoral Fellow† |
| KONDO, Naoko | Secretary |


Nonequilibrium properties of low-dimensional correlated electron systems are investigated from different aspects. Among them, photoinduced transitions are now widely achieved between metals and insulators, between paraelectric and ferroelectric phases, among nonmagnetic, paramagnetic and ferromagnetic phases, and so on.[1)] Most of them are realized by changing the temperature also. Here, we focus on a quantum phase transition between neutral quantum- paraelectric and ionic (anti)ferroelectric ground (*i.e.*, zero temperature) states, where photoinduced dynamics are experimentally demonstrated to be different from ordinary ones. In addition, we continue the research for the mechanisms of different rectifying actions. Here, we employ nonequilibrium Green's functions to elucidate differences between strongly-correlated and weakly-correlated insulators.

## 1. Enhanced Coherent Dynamics near a Quantum Phase Transition[2)]

A quantum phase transition between neutral quantum-paraelectric and ionic antiferroelectric phases is realized in mixed-stack charge-transfer complexes composed of 4,4'-dimethyltetrathiafulvalene (DMTTF) and tetrahalo-*p*-benzoquinones ($QBr_nCl_{4-n}$). Recently, photoinduced reflectivity changes are reported. The reflectivity in the energy range where it is sensitive to the ionicity change shows a large-amplitude oscillation near the quantum phase transition point. Then, nonequilibrium dynamics is studied near the quantum phase transition point in the one-dimensional quantum Blume-Emery-Griffiths model. Its pseudospin component $S^z$ represents an electric polarization, and $(S^z)^2$ corresponds to ionicity. This model is one-dimensional and does not distinguish between ferroelectric and antiferroelectric phases. The time-dependent Schrödinger equation is solved for the exact many-body wave function in the quantum-paraelectric phase. After impact force is introduced on a polarization locally in space and time, polarizations [Figure 1(a)] and ionicity [Figure 1(b)] coherently oscillate. The oscillation amplitudes are large near the quantum phase transition point. The dependences of these oscillation amplitudes on the total-energy increment $\Delta E$ are shown in Figure 2 for different quantum-tunneling amplitudes $h$.

The energy supplied by the impact flows linearly into these oscillations, so that the nonequilibrium behavior is uncooperative.

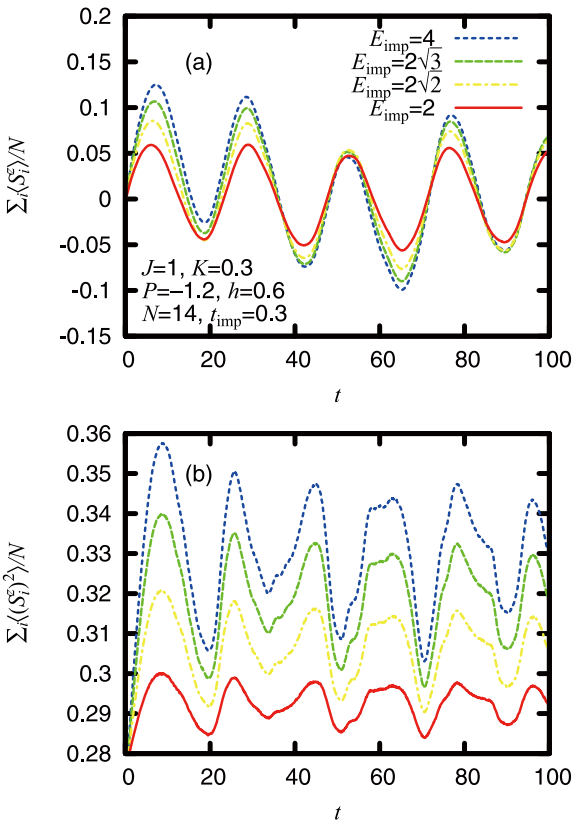


**Figure 1.** (a) Spatial average of electric polarization $S^z$ and (b) spatial average of ionicity $(S^z)^2$, as a function of time $t$, after impact force of strength $E_{imp}$ is locally introduced on a polarization.

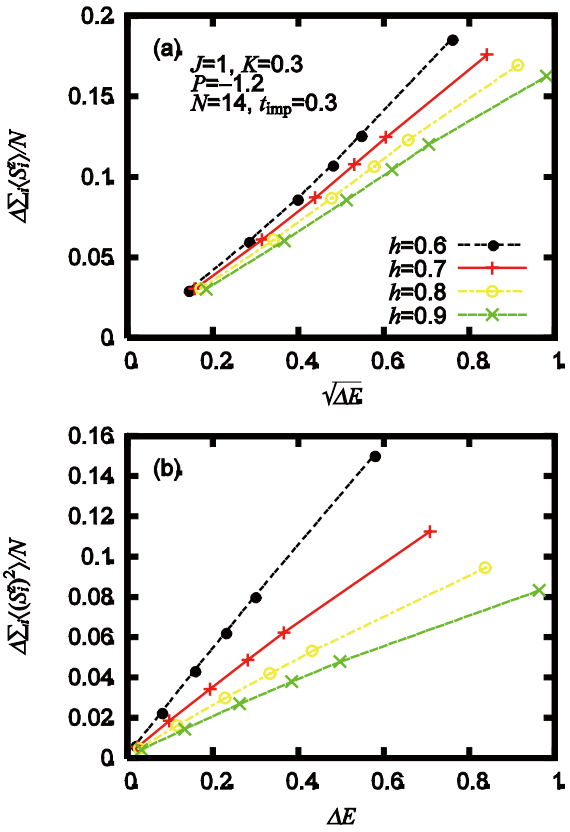


**Figure 2.** (a) Amplitude of oscillation in spatial average of electric polarization $S^z$, as a function of square root of energy supplied, and (b) amplitude of oscillation in spatial average of ionicity $(S^z)^2$, as a function of energy supplied $\Delta E$. The quantity $h$ denotes the quantum-tunneling amplitude.

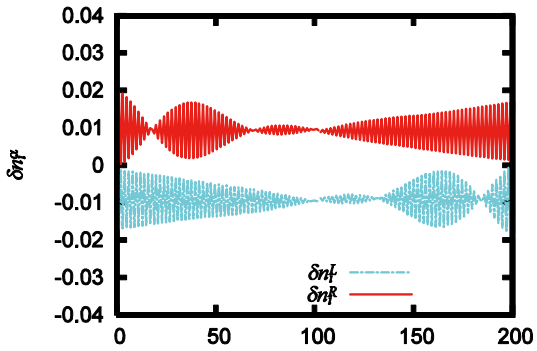


**Figure 3.** Nonequilibrium part of charge density due to coupling with left electrode, $\delta n^{\mathrm{L}}{}_i$ (light blue), and that with right electrode, $\delta n^{\mathrm{R}}{}_i$ (red), for Mott insulator with left-going bias.

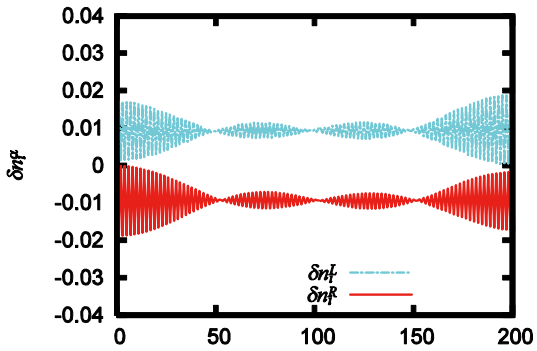


**Figure 4.** Nonequilibrium part of charge density due to coupling with left electrode, $\delta n^{\mathrm{L}}{}_i$ (light blue), and that with right electrode, $\delta n^{\mathrm{R}}{}_i$ (red), for Mott insulator with right-going bias.

## 2. Nonequilibrium Green's Functions for Rectification at Metal–Insulator Interfaces[3)]

The suppression of rectification at metal–Mott-insulator interfaces, which was previously shown by numerical solutions to the time-dependent Schrödinger equation and experiments on real devices, is reinvestigated theoretically using nonequilibrium Green's functions. The one-dimensional Hubbard model is used for a Mott insulator. The effects of attached metallic electrodes are incorporated into the self-energy. A scalar potential originating from work-function differences and satisfying the Poisson equation is added to the model. For electron density, we decompose it into three parts. One is obtained by integrating the local density of states over energy to the midpoint of the electrodes' chemical potentials.

The others, obtained by integrating lesser Green's functions, are due to couplings with the electrodes and correspond to an inflow and an outflow of electrons (Figures 3 and 4). In Mott insulators, incoming electrons and holes are extended over the whole system, avoiding further accumulation of charges relative to that in the case without bias. Furthermore, the inflow and the outflow of electrons are insensitive to the polarity of the bias. This induces collective charge transport and results in the suppression of rectification.

### References

1) K. Yonemitsu and K. Nasu, *Phys. Rep.* **465**, 1–60 (2008).
2) K. Yonemitsu, *Phys. Rev. B* **78**, 205102 (5 pages) (2008).
3) K. Yonemitsu, *J. Phys. Soc. Jpn.* **78**, 054705 (8 pages) (2009).

### Award

YAMASHITA, Yasufumi; Young Scientist Award of the Physical Society of Japan.

* Present Address: General Studies, College of Engineering, Nihon University, Koriyama, Fukushima 963-8642
† Present Address: Japan Science and Technology Agency, Chiyoda-ku, Tokyo 102-0075

# Theoretical Studies on Condensed Phase Dynamics

**Department of Theoretical and Computational Molecular Science**
**Division of Computational Molecular Science**

| | |
|---|---|
| SAITO, Shinji | Professor |
| KIM, Kang | Assistant Professor |
| HIGASHI, Masahiro | IMS Fellow |
| KOBAYASHI, Chigusa | Post-Doctoral Fellow |
| YAGASAKI, Takuma | Post-Doctoral Fellow |
| SUMIKAMA, Takashi | Post-Doctoral Fellow |
| IMOTO, Sho | Graduate Student* |
| UENO, Harumi | Secretary |


Liquids and biological systems show complicated dynamics because of their structural flexibility and dynamical hierarchy. Understanding these complicated dynamics is indispensable to elucidate chemical reactions and relaxation in solutions and functions of proteins. We have been investigating complex dynamics in supercooled liquids[1–3] and chemical reactions in biological systems using molecular dynamics simulation and electronic structure calculation. In addition, we have been analyzing liquid dynamics by using multi-dimensional spectroscopy.[4,5]

## 1. Multiple Time Scales Hidden in Heterogeneous Dynamics of Glass-Forming Liquids[1]

A multi-time probing of density fluctuations is introduced to investigate hidden time scales of heterogeneous dynamics in glass-forming liquids. Molecular-dynamics simulations for simple glass-forming liquids are performed and a three-time correlation function is numerically calculated for general time intervals. It is demonstrated that the three-time correlation function is sensitive to the heterogeneous dynamics and that it reveals couplings of correlated motions over a wide range of time scales. Furthermore, the time scale of the heterogeneous dynamics $\tau_{hetero}$ is determined by the change in the second time interval in the three-time correlation function. The present results show that the time scale of the heterogeneous dynamics $\tau_{hetero}$ becomes larger than the $\alpha$-relaxation time at low temperatures and large wavelengths. We also find a dynamical scaling relation between the time scale $\tau_{hetero}$ and the length scale $\xi$ of dynamical heterogeneity as $\tau_{hetero} \sim \xi^z$ with $z = 3$.

## 2. Slow Dynamics in Random Media: Crossover from Glass to Localization Transition[2]

We study slow dynamics of particles moving in a matrix of immobile obstacles using molecular dynamics simulation. The glass transition point decreases drastically as the obstacle density increases. At higher obstacle densities, dynamics of mobile particles changes qualitatively from glass-like to a Lorentz-gas-like relaxation. This crossover is studied by the density correlation functions, non-ergodic parameters, mean square displacement, and nonlinear dynamic susceptibility. Our finding is qualitatively consistent with results of recent numerical and theoretical studies on various spatially heterogeneous systems. Furthermore, we show that slow dynamics is surprisingly rich and sensitive to the obstacle configurations. Especially, reentrant transition is observed for a particular configuration, though its origin is not directly linked to the similar prediction based on the mode-coupling theory.

## 3. Conformational Changes and Fluctuations of Molecular Switch Ras

Ras superfamily works as a molecular switch for cell growth. Ras is cycled between two states of guanine nucleotide, the GTP- and GDP-bound states, by hydrolysis. Ras binds to effectors for regulation of cell proliferation in the GTP-bound state, whereas it is inactivated in the GDP-bound state. X-ray crystallography studies revealed conformational changes of two regions, *i.e.* switch I and switch II, around a nucleotide binding site in these two states. We analyze the conformational

changes and fluctuations between these states by carrying out molecular dynamics (MD) simulation. We find that the change in the coordinations of Thr35-$Mg^{2+}$ and Gly60-γ-phosphate due to the hydrolysis of GTP induces the changes in the conformations of sidechains as well as the backbone in the GTP- and GDP-bound states. We perform the principle coordinate analysis of the structural change between these states and indeed find the important structural change arising from the switch regions.

In addition to the GTP-bound state with the function of the cell growth, another GTP-bound state with different conformation has been observed experimentally. The GTP-bound state with the function is called state 2, while the other state is referred to as state 1. It is known that state 2 is a predominant form of Ras and interacts with effectors. $^{31}P$ NMR spectroscopy of some mutants shows the absence of the coordination of Thr35-$Mg^{2+}$ in state 1. It is also shown in X-ray structural analysis that the coordination of Gly60-γ-phosphate is lost in the state 1 of another mutant. We investigate the conformational changes and fluctuations in these two kinds of state 1 by using MD simulation. It is found that the breaking of the coordination of Thr35-$Mg^{2+}$ causes the large scale structural change in the switch I region followed by the steric hindrance between Pro34 and γ-phosphate and then the break of hydrogen bond between ribose in GTP and switch I region. We also find that the conformational fluctuation in the switch I region is substantially large in state 1. We show that the global structural changes of loop4 and α2 helix in the switch II region are induced by the loss of the coordination between Gly60 and γ-phosphate. The presence of multiple states with different conformations in the GTP-bound state is consistent with the experimentally observed interconversion between multiple conformations and with the low affinity to effectors.

We also analyze the GAP-GTP-bound state to understand the role of GAP. We find that the binding of GAP significantly suppressed the unnecessary thermal motions of the water molecule which is involved in the hydrolysis of GTP.

In addition to the above analyses based on MD simulation, we are currently analyzing the reaction pathway of hydrolysis of GTP in the GAP-GTP-bound state, by using the so-called QM/MM method.

## 4. Molecular Dynamics Simulation of Nonlinear Spectroscopies of Intermolecular Motions in Liquid Water[4,5)]

Water is the most extensively studied of liquids because of both its ubiquity and its anomalous thermodynamic and dynamic properties. The properties of water are dominated by hydrogen bonds and hydrogen bond network rearrangements. Fundamental information on the dynamics of liquid water has been provided by linear infrared (IR), Raman, and neutron-scattering experiments; molecular dynamics simulations have also provided insights. Recently developed higher-order nonlinear spectroscopies open new windows into the study of the hydrogen bond dynamics of liquid water. For example, the vibrational lifetimes of stretches and a bend, intramolecular features of water dynamics, can be accurately measured and are found to be on the femtosecond time scale at room temperature. Higher-order nonlinear spectroscopy is expressed by a multi-time correlation function, whereas traditional linear spectroscopy is given by a one-time correlation function. Thus, nonlinear spectroscopy yields more detailed information on the dynamics of condensed media than linear spectroscopy. In this Account, we describe the theoretical background and methods for calculating higher-order nonlinear spectroscopy; equilibrium and non-equilibrium molecular dynamics simulations, and a combination of both, are used. We also present the intermolecular dynamics of liquid water revealed by fifth-order two-dimensional (2D) Raman spectroscopy and third order IR spectroscopy. 2D Raman spectroscopy is sensitive to couplings between modes; the calculated 2D Raman signal of liquid water shows large anharmonicity in the translational motion and strong coupling between the translational and librational motions. Third-order IR spectroscopy makes it possible to examine the time-dependent couplings. The 2D IR spectra and three-pulse photon echo peak shift show the fast frequency modulation of the librational motion. A significant effect of the translational motion on the fast frequency modulation of the librational motion is elucidated by introducing the "translation-free" molecular dynamics simulation. The isotropic pump-probe signal and the polarization anisotropy decay show fast transfer of the librational energy to the surrounding water molecules, followed by relaxation to the hot ground state.

### Reference

1) K. Kim and S. Saito, *Phys. Rev. E* **79**, 060501(R) (4 pages) (2009).
2) K. Kim, K. Miyazaki and S. Saito, *Europhys. Lett.* **88**, 36002 (5 pages) (2009).
3) A. Furukawa, K. Kim, S. Saito and H. Tanaka, *Phys. Rev. Lett.* **102**, 016001 (4 pages) (2009).
4) T. Yagasaki and S. Saito, *Acc. Chem. Res.* **42**, 1250–1259 (2009).
5) T. Yagasaki, J. Ono and S. Saito, *J Chem. Phys.* **131**, 164511 (11 pages) (2009).

* carrying out graduate research on Cooperative Education Program of IMS with Nagoya University

# Theoretical Study on Molecular Excited States and Chemical Reactions

**Department of Theoretical and Computational Molecular Science**
**Division of Computational Molecular Science**

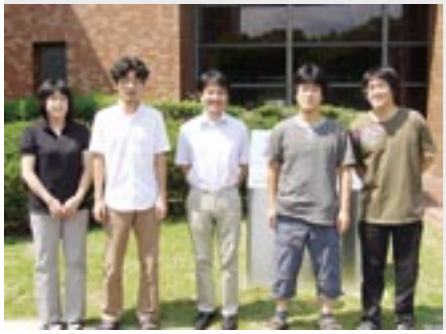

| | |
|---|---|
| EHARA, Masahiro | Professor |
| FUKUDA, Ryoichi | Assistant Professor |
| TASHIRO, Motomichi | IMS Research Assistant Professor |
| VONGACHARIYA, Arthit | Research Fellow |
| KAWAGUCHI, Ritsuko | Secretary |


Molecules in the excited states show characteristic photophysical properties and reactivity. We investigate the molecular excited states and chemical reactions which are relevant in chemistry, physics, and chemical biology with developing the highly accurate electronic structure theory. We are also interested in the excited-state dynamics and energy relaxation so that we also develop the methodology of large-scale quantum dynamics. In this report, we report our recent studies on the development of the active-space method,[1] molecular excited states,[2–4] in particular the inner- shell spectroscopy[3,4] and catalytic reaction on surface.[5]

## 1. Development of Active-Space Method[1]

Radicals show characteristic spectroscopic properties and reactivity in their ground and excited states. Since they are unstable and short-lived, their spectroscopic properties and reactions have to be examined through suitably designed experimental procedures, such as flash photolysis and matrix isolation spectroscopy, to mention a few examples. Excellent experimental techniques using argon and solid parahydrogen matrices have been developed for this purpose. Thanks to these and related advances, a large amount of experimental data has been accumulated for radicals, and a highly accurate theoretical analysis has become an indispensable tool for obtaining a detailed interpretation of these data.

In this work, we have developed the active-space method based on the SAC-CI method and applied the theory to the molecular spectroscopy of open-shell systems. The low-lying valence excited states of four open-shell triatomic molecules, CNC, $C_2N$, $N_3$, and NCO, were investigated using the electron-attached (EA) and ionized (IP) SAC-CI general-*R* as well as the full and active-space EA and IP EOMCC methods. A comparison was made with experiment and with the results of the completely renormalized (CR) CC calculations with singles, doubles, and non-iterative triples defining the CR-CC (2,3) approach. Adiabatic excitation energies of the calculated states were in reasonable agreement with the experimental values, provided that the 3-particle–2-hole (3p-2h) components in the electron attaching operator, as in the EA SAC-CI SDT-*R* and EA EOMCCSD(3p-2h) approaches, are included in the calculations for the excited states of $C_2N$ and CNC which have a predominantly two-electron character. The results also revealed that the active-space EA/IP EOMCC schemes with up to 3p-2h/3h-2p excitations are able to accurately reproduce the results of their much more expensive parent methods while requiring significantly less computational effort. Furthermore, the more "black-box" CR-CC(2,3) approach calculated the lowest state of each symmetry with the same accuracy as that obtained with the EA/IP SAC-CI SDT-*R* and EA/IP EOMCCSD (3p-2h/3h-2p) methods, confirming the significance of higher-order correlation effects in obtaining an accurate description of excited states of radicals, particularly the valence excited states of the CNC and $C_2N$ species dominated by two-electron processes. Table 1 summarizes the results of the ground and excited states of $C_2N$.

**Table 1.** Spectroscopic constants of the ground and excited states of $C_2N$.

| State | Method | Exc. level | $R_{CC}$ (Å) | $R_{CN}$ (Å) | $T_e$ (eV) |
|---|---|---|---|---|---|
| X $^2\Pi$ | SD-*R* | 1 | 1.405 | 1.191 | --- |
| | SDT-*R*{4,4} | 1 | 1.400 | 1.185 | --- |
| | Expt. | | --- | | --- |
| A $^2\Delta$ | SD-*R* | 2 | 1.352 | 1.185 | 6.004 |
| | SDT-*R*{4,4} | 2 | 1.315 | 1.207 | 2.837 |
| | Expt. | | --- | | 2.636 |
| B $^2\Sigma^-$ | SD-*R* | 2 | 1.354 | 1.188 | 7.632 |
| | SDT-*R*{4,4} | 2 | 1.302 | 1.223 | 3.640 |
| | Expt. | | --- | | 2.779 |
| C $^2\Sigma^+$ | SD-*R* | 2 | 1.341 | 1.192 | 6.578 |
| | SDT-*R*{4,4} | 2 | 1.311 | 1.214 | 3.594 |
| | Expt. | | --- | | 3.306 |

## 2. Relativistic Effects in *K*-Shell Ionizations: SAC-CI General-*R* Study Based on the DK2 Hamiltonian[3]

Core-electron binding energies (CEBEs) contain infor-

mation not only about inner-core electrons but also about valence electrons and chemical bonds. Extensive experimental studies have provided the CEBEs of numerous molecules. Siegbahn *et al.* summarized the electron spectroscopy for chemical analysis (ESCA) data in 1969 and Bakke *et al.* reported further ESCA data in 1980. They also clarified the important chemical implications involved in the CEBE data. The recent development of high-resolution soft X-ray photoelectron spectroscopy (XPS) has enabled accurate experimental observations of the CEBEs, resolving the vibrational structure.

It is now generally recognized that the relativistic effect is important in chemistry in particular for the molecular properties of the heavy elements. The methodologies of relativistic quantum chemistry have been developed and established. The relativistic effect is also important in core-electron processes. Although the spin-orbit splitting of the inner-shell P and D states has been intensively investigated, the relativistic effect has not been so much focused in the accurate calculation of the CEBEs for the heavy elements. Most calculations including both electron correlations and relativistic effect have been performed for molecules containing first-row atoms except for the recent work of Barysz and Leszczynski for the rare gas atoms.

In this work, we investigated the relativistic effects in the CEBEs of molecules containing the second-row atoms, Si, P, S, and Cl as well as the F atom. We performed the SAC-CI general-*R* calculations based on the spin-free part of the second-order Douglass-Kroll-Hess (DK2) Hamiltonian.[3] Table 2 summarizes the results of the relativistic and non-relativistic SAC-CI calculations. The relativistic effect in the CEBEs of the second-row atoms was found to be 4–9 eV. The effect was mostly overestimated by the Koopmans' theorem and was reduced to the extent of 0.15–0.4 eV by including the orbital relaxation and electron correlations.

**Table 2.** Calculated and observed Si, P, S, and Cl 1s CEBE (eV).

| Mol. | Exptl. | Rel. SAC-CI | Non-Rel. SAC-CI | Rel. effect (eV) SAC-CI | Koopmans' |
|---|---|---|---|---|---|
| $\underline{Si}H_4$ | 1847.1 | 1848.24 | 1843.96 | 4.28 | 3.97 |
| $\underline{P}H_3$ | 2150.5 | 2151.25 | 2146.32 | 4.93 | 5.30 |
| $H_2\underline{S}$ | 2478.5 | 2479.51 | 2472.98 | 6.53 | 6.94 |
| O$\underline{C}$S | 2480.3 | 2481.84 | 2475.06 | 6.78 | 6.93 |
| $CH_3\underline{Cl}$ | 2829.4 | 2832.15 | 2823.35 | 8.80 | 8.95 |

## 3. Theoretical Study of the Methanol Dehydrogeneation Reaction on Pt and Ag Surfaces/Clusters[5]

The mechanism of the methanol dehydrogenation reaction on a Pt surface has been investigated using the dipped adcluster model (DAM) combined with density functional theory (DFT) calculations. Reaction pathways starting from CH and OH dissociations (Figure 1), both of which were proposed experimentally, but, not fully understood, have been examined.

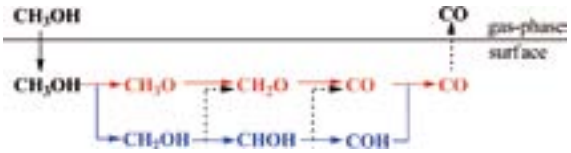


**Figure 1.** Reaction pathways of the dehydrogenation of $CH_3OH$ to CO.

Starting from O–H bond scission, methanol decomposes to form CO exothermically on the Pt surface, where the Pt-dσ orbital effectively interacts with the O–H antibonding orbital. The donative interaction of the Pt dσ orbitals was found to be important for catalytic activation on the Pt surface. Figure 2 shows the overall energy diagram of the methanol dehydrogenation reaction starting. The reaction pathway starting from C–H bond scission has a larger activation barrier and, therefore, is less kinetically favorable. Electron transfer from the bulk, which is included in the present DAM calculation, plays an important role in the reaction pathway from O–H bond scission, in particular for the dehydrogenation of formaldehyde. On the other hand, the Ag surface has been shown to be effective for formaldehyde synthesis, because formaldehyde desorbs spontaneously from the Ag surface. The present reaction has also been examined and discussed in view of the nanoscale clusters and nanorods.

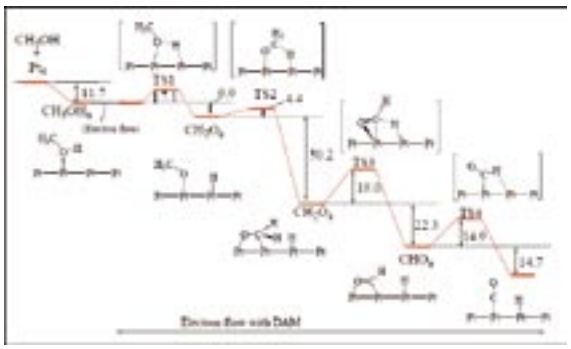

**Figure 2.** Overall energy diagram of methanol dehydrogenation starting from OH bond dissociation.

### References


1) M. Ehara, J. R. Gour and P. Piecuch, *Mol. Phys.* **107**, 871–880 (2009).
2) S. Arulmozhiraja, M. Ehara and H. Nakatsuji, *J. Chem. Phys.* **129**, 174506 (8 pages) (2008).
3) M. Ehara, K. Kuramoto and H. Nakatsuji, *Chem. Phys.* **356**, 195–198 (2009).
4) K. Ueda, R. Puttner, N. A. Cherepkov, F. Gel'mukhanov and M. Ehara, *Eur. Phys. J.* **169**, 95–107 (2009).
5) T. Watanabe, M. Ehara, K. Kuramoto, H. Nakatsuji, *Surf. Sci.* **603**, 641–646 (2009).


### Award

EHARA, Masahiro; APATCC (Asia-Pacific Association of Theoretical & Computational Chemists) 2009 Pople Medal.

# Development of New Algorithms for Molecular Dynamics Simulation and Its Application to Biomolecular Systems

**Department of Theoretical and Computational Molecular Science**
**Division of Computational Molecular Science**

OKUMURA, Hisashi — Associate Professor
KAWAGUCHI, Ritsuko — Secretary

## 1. Temperature and Pressure Dependence of Alanine Dipeptide Studied by Multibaric-Multithermal Molecular Dynamics Simulations[1)]

We applied the multibaric-multithermal (MUBATH) molecular dynamics (MD) algorithm to an alanine dipeptide in explicit water (Figure 1). The MUBATH MD simulation covered a wide range of conformational space and sampled the states of $P_{II}$, $C_5$, $\alpha_R$, $\alpha_P$, $\alpha_L$, and $C_7^{ax}$. On the other hand, the conventional isobaric-isothermal simulation was trapped in local-minimum free-energy states and sampled only a few of them. Temperature and pressure dependences of the population of these states were investigated by the MUBATH MD simulations as shown in Figure 2. Such temperature and pressure dependences by molecular simulations were calculated for the first time. We calculated the partial molar enthalpy difference $\Delta H$ and partial molar volume difference $\Delta V$ among these states by the MUBATH simulation using the AMBER parm99 and AMBER parm96 force fields and two sets of initial conditions as listed in Tables 1 and 2. We compared these results with those from Raman spectroscopy experiments. The Raman spectroscopy data of $\Delta H$ for the $C_5$ state against the $P_{II}$ state agreed with both MUBATH data with the AMBER parm96 and parm99 force fields. The partial molar enthalpy difference $\Delta H$ for the $\alpha_R$ state and the partial molar volume difference $\Delta V$ for the $C_5$ state by the Raman spectroscopy agreed with those for the AMBER parm96 force field. On the other hand, $\Delta V$ for the $\alpha_R$ state by the Raman spectroscopy was consistent with our AMBER-parm99 force-field result. All the experimental results fall in between those of simulations using AMBER parm96 and parm99 force fields, suggesting that the ideal force field parameter lie between those of AMBER parm96 and parm99.

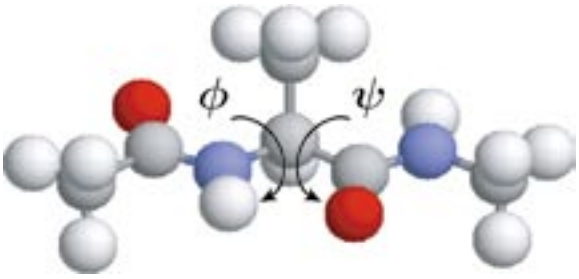


**Figure 1.** The initial conformations of alanine dipeptide for the MD simulation.

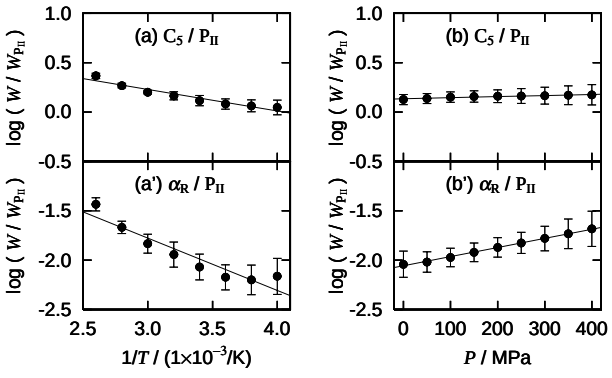


**Figure 2.** The population ratios of (a) the $C_5$ state and (a') the $\alpha_R$ state against the $P_{II}$ state as functions of the inverse of temperature $1/T$ at constant pressure of $P$ = 0.1 MPa. The population ratios of (b) the $C_5$ state and (b') the $\alpha_R$ state against the $P_{II}$ state as functions of pressure $P$ at constant temperature of $T$ = 298 K.

**Table 1.** Differences $\Delta H$/(kJ/mol) in partial molar enthalpy of the $C_5$, and $\alpha_R$ states from that of the $P_{II}$ state calculated by the MUBATH MD simulations. Raman experimental data are also listed.

| State | AMBER 96 | AMBER 99 | Raman exp. |
|---|---|---|---|
| $C_5$ | 1.8±0.5 | 3.6±2.2 | 2.5±0.3 |
| $\alpha_R$ | 4.4±1.1 | –1.5±2.0 | 4.4±1.5 |

**Table 2.** Differences $\Delta V$/(cm$^3$/mol) in partial molar volume of the $C_5$, and $\alpha_R$ states from that of the $P_{II}$ state calculated by the MUBATH MD simulations. Raman experimental data are also listed.

| State | AMBER 96 | AMBER 99 | Raman exp. |
|---|---|---|---|
| $C_5$ | –0.3±0.7 | 1.5±0.9 | 0.1±0.3 |
| $\alpha_R$ | –2.3±1.3 | 1.8±0.8 | 1.1±0.2 |

## 2. Partial Multicanonical Algorithm for Molecular Dynamics and Monte Carlo Simulations[2)]

Partial multicanonical algorithm is proposed for molecular dynamics and Monte Carlo simulations. The partial multicanonical simulation samples a wide range of a part of the potential energy terms which is necessary to sample the conformational space widely, whereas a wide range of total potential energy is sampled in the multicanonical algorithm. Thus, one can concentrate the effort to determine the weight factor only on the important energy terms in the partial multicanonical simulation. The partial multicanonical, multicanonical, and canonical molecular dynamics algorithms were applied to an alanine dipeptide in explicit water solvent. The canonical simulation sampled the states of $P_{II}$, $C_5$, $\alpha_R$, and $\alpha_P$. The multicanonical simulation covered the $\alpha_L$ state as well as these states. The partial multicanonical simulation also sampled the $C_7^{ax}$ state in addition to the states which were sampled by the multicanonical simulation as shown in Figure 3. In the partial multicanonical simulation, furthermore, backbone dihedral angles $\phi$ and $\psi$ rotated more frequently than in the multicanonical and canonical simulations. These results mean that the partial multicanonical algorithm has higher sampling efficiency than the multicanonical and canonical algorithms.

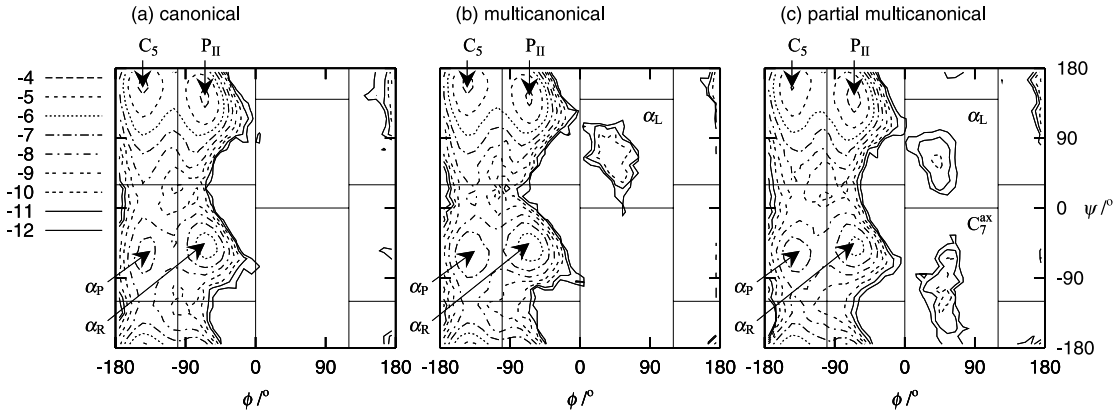


**Figure 3.** Contour maps of the logarithms of the probability distributions $\log P_{NVT}(\phi,\psi)$ of the backbone dihedral angles $\phi$ and $\psi$ at $T$ = 300 K obtained (a) by the canonical MD simulation, (b) by the reweighting techniques from the results of the multicanonical MD simulation, and (c) by the reweighting techniques from the results of the partial multicanonical MD simulation.

### References

1) H. Okumura and Y. Okamoto, *J. Phys. Chem. B* **112**, 12038–12049 (2008).

2) H. Okumura, *J. Chem. Phys.* **129**, 124116 (9 pages) (2008).

# Theory and Computation of Reactions and Properties in Solutions and Liquids

**Department of Theoretical and Computational Molecular Science**
**Division of Computational Molecular Science**

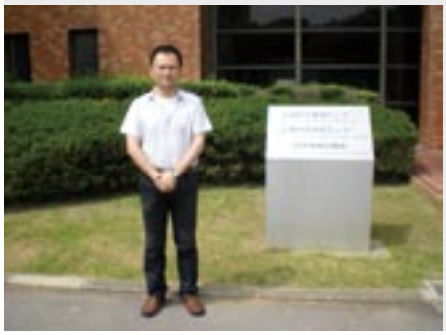

ISHIDA, Tateki Assistant Professor

We focus on the projects both on ultrafast photoinduced reaction and on ionic liquids. The project on photoinduced reaction processes in solution focuses on the development of a theoretical method to describe solvent motion and dynamics around a solute molecule in short-time region. Also, it includes the application of the developed theoretical treatment to solvation processes and excited-state intramolecular processes in Betaine dye molecule solution. On the other hand, the project on ionic liquids is collaborating work with the experimental studies by Prof. Shirota at Chiba University.

## 1. Solvent Motions and Solvation Processes in a Short-Time Regime: Effects on Excited-State Intramolecular Processes in Solution[1)]

We propose a method for treating equation of motions for atoms taking into account the inertial term with an interaction site model for capturing solvent dynamics attributed to solvent motions in a short-time regime, $t < 100$ fs. We show a prescription for solving the equation which governs the development of the fluctuation of solvent number density with the inertial term, and, also, the procedure is applied to the study of solvation dynamics of the simplest betaine dye molecule pyridinium *N*-phenoxide in water in the excited state. It is shown that the coupling between solvation and a fast intramolecular reaction such as charge transfer is likely to play an important role in solvation dynamics of the simplest betaine.

## 2. Atom Substitution Effects of $[XF_6]^-$ in Ionic Liquids. 1. Experimental Study[2)]

We have investigated the interionic vibrational dynamics of 1-butyl-3-methylimidazolium cation ($[BMIm]^+$) based ionic liquids with the anions of $[PF_6]^-$, $[AsF_6]^-$, and $[SbF_6]^-$ as well as the static physical properties, such as shear viscosity and liquid density. Shear viscosity for the ionic liquids becomes lower with the heavier atom anion: [BMIm][$PF_6$] > [BMIm][$AsF_6$] > [BMIm][$SbF_6$]. Femtosecond optically heterodyne-detected Raman-induced Kerr effect spectroscopy has been used to observe the interionic vibrational dynamics of ionic liquids. The interionic vibration in the frequency region of less than 50 $cm^{-1}$ clearly shows the heavy atom substitution effect; that is, the heavy atom substitution of $[XF_6]^-$ critically affects the interaction-induced motion.

## 3. Atom Substitution Effects of $[XF_6]^-$ in Ionic Liquids. 2. Theoretical Study[3)]

We have carried out the molecular dynamics simulations for 1-butyl-3-methylimidazolium cation based ILs ([BMIm][$PF_6$], [BMIm][$AsF_6$], and [BMIm][$SbF_6$]) including the calculations of density of state (DOS) profiles, polarizability time correlation function (TCF), and Kerr spectra (with the development of the force fields of $[AsF_6]^-$ and $[SbF_6]^-$ by an ab initio calculation). From these computational studies, we find that the contribution of the reorientation of cations and anions mainly governs the Kerr spectrum profile in all three ILs, while the contribution of the collision-induced and cross terms, which are related to translational motions including coupling with librational motion, is not large at higher frequencies than 50 $cm^{-1}$. In addition, it is emphasized in this study that atomic mass effects in ILs are accessible through a complementary approach of both experimental and theoretical approaches.

### References

1) T. Ishida, *J. Phys. Chem. B* **113**, 9255–9264 (2009).
2) H. Shirota, K. Nishikawa and T. Ishida, *J. Phys. Chem. B* **113**, 9831–9839 (2009).
3) T. Ishida, K. Nishikawa and H. Shirota, *J. Phys. Chem. B* **113**, 9840–9851 (2009).

# Visiting Professors

Visiting Professor
**TAKETSUGU, Tetsuya** *(from Hokkaido University)*

Ab Initio Dynamics Study of Excited-State Chemical Reactions

We have developed an ab initio molecular dynamics (AIMD) program code for excited-state reaction dynamics, combined with the quantum chemistry program packages, MOLPRO and GAMESS, and applied it to several significant photoreactions at the state-averaged CASSCF level. In the current code, non-adiabatic transitions are treated by the Tully's surface hopping algorithm, while the solvent effects are treated by QM/MM approach. The applications include the excited-state dynamics of 7-azaindole-$H_2O$ cluster (excited-state proton transfer), coumarin 151 in water solution (large solvent effects), cytosine (examination of photostability), photo-isomerization of azobenzene (examination of reaction pathways), dissociative recombination reactions of small molecules (surface hopping dynamics), and photodissociation of $CH_3I$ (spin-orbit coupling effects). Through these applications, the code has been extended for general use to examine excited-state dynamics of real molecular system.

Visiting Associate Professor
**NAKAJIMA, Takahito** *(from The University of Tokyo)*

Development of Large-Scale Molecular Theory

With the emergence of peta-scale computing platforms we are entering a new period of the molecular simulation. The computer simulations can be carried out for larger, more complex, and more realistic molecular systems such as nano- and bio-materials than ever before. To make the most of the computer resource, we should achieve some breakthroughs of conventional theoretical approaches. We have proposed several efficient molecular theories to treat large molecular systems accurately via relativistic and non-relativistic treatments. These approaches include several types of auxiliary basis approaches, such as the pseudospectral method, the resolution of the identity method, the augmented plane-waves method, and the augmented finite-elements method. We expect that these approaches will be capable of the clarification of chemical phenomena in nano- and bio-materials with the help of the next generation supercomputer.

Visiting Associate Professor
**HAYASHI, Shigehiko** *(from Kyoto University)*

Molecular Simulation Studies of Protein Functions

Protein functional activities involve dynamic molecular conformational changes of complex protein systems. Hence molecular dynamics underlying functional activities are necessary to be revealed for understanding of molecular nature of protein functions. We performed molecular dynamics (MD) simulations on photochemical dynamics of rhodopsins (Rh) and ligand migration dynamics in myoglobin (Mb). We carried out an ab initio quantum mechanical/molecular mechanical MD simulation for the retinal photoisomerization processes in Rh, and revealed a dynamic regulation mechanism for the fast photoisomerization. We also examined the ligand migration dynamics in Mb by a meta-dynamics simulation and a linear response theory, and identified remarkable collective protein motions coupled to the transient ligand migrations through the migration channels.